Nanoarchitectonics
http://ojs.wiserpub.com/index.php/NAT/

UNIVERSAL WISER PUBLISHER

Research Article

Growth and Characterization of Al (111) Thin Film on Piezoelectric Wafers for SAW Device Fabrication for Space Applications

Manish Kumar Sahu[1*], Ajaya Kumar PS[1], Chiranjit Karmakar[1], Gunjan Rastogi[2], R. K. Kaneriya[1], R. B. Upadhyay[1]

[1]Microelectronics Group, Space Applications Centre, ISRO, Ahmedabad, India
[2]Thermal Systems Group, UR Rao Satellite Centre, ISRO, Bengaluru, India
E-mail: manish11@sac.isro.gov.in

Received: 15 June 2022; **Revised:** 6 August 2022; **Accepted:** 16 August 2022

Abstract: Surface Acoustic Wave (SAW) filters provide precise frequency filtering in RF and IF range with a tiny footprint. Metallic thin films are the essence of such modern SAW filter technology. However, SAW filters realized using NiCr/Al thin films are limited to power levels of ~5 dBm at RF frequencies. This limitation on power level is due to the acousto-migration phenomenon in thin films at higher power levels. In order to enhance the power durability of SAW filters, the preferred oriented growth of Al along (111) crystallographic direction is one of the methods to reduce acousto-migration. This paper explores the growth and characterization of different metallization schemes (NiCr/Al & Ti/Al) on different piezoelectric wafers to achieve oriented Al (111) film growth. Metallic thin films were deposited using electron beam evaporation technique. High Resolution X-Ray Diffraction (HR-XRD) and Four Point Probe Method were used for crystallographic characterization and Sheet Resistance (SR) measurement, respectively. Atomic Force Microscopy (AFM) and surface profiler were used to characterize the surface morphology of the deposited films. FWHM of 4.12 degree of rocking curve on Al (111) peak has been achieved for Ti/Al metal film deposited on ST-X Quartz piezoelectric wafer along with low sheet resistance of 124 mΩ/sq. A deposition rate of 1 Å/s for Ti and 7 Å/s for Al at a deposition temperature of 100 °C gave the best FWHM value for Al (111) orientation on ST-X Quartz wafer. Space qualification tests were also successfully performed on Ti/Al metalized wafers under extreme environmental conditions. The results obtained in this work demonstrate the suitability of Ti as an under layer to grow preferred oriented Al film along (111) orientation and thus to be used in the fabrication of high-power SAW devices for space applications.

***Keywords*:** SAW filters, electron beam evaporation, metallic thin films, X-ray diffraction, space applications

1. Introduction

SAW filters are widely used in payload sub-systems for precise frequency selection in satellites. They are also extensively used in telecommunications [1], radar technology, and medical applications [2]. SAW filter consists of thin film metal electrodes patterned on top of piezoelectric wafers. These patterned electrodes (also known as Inter Digital Transducers) convert the incoming electrical signal into acoustic energy by virtue of the piezoelectric effect. The

DOI: https://doi.org/10.37256/nat.4120231624

acoustic wave thus generated at the input Inter-Digital Transducer (IDT) is suitably processed and converted back to an electrical signal at the output IDT by the inverse piezoelectric effect. Depending on different piezoelectric wafers, SAW filters can be realized for frequencies ranging from 10 MHz to 3 GHz [3].

SAW filter fabrication requires an ultra-thin NiCr (adhesive layer) to be grown on top of a piezoelectric wafer on top of which Al thin film is grown. With increasing demands for device miniaturization, the power handling capacity of SAW filters should be increased accordingly to process data faster [4]. However, the power durability of SAW filters having NiCr/Al metallization is limited. Acousto-migration is the primary mode of failure of SAW devices at higher power levels [5]. With rising power levels, the amplitude of SAW increases and leads to the migration of metal atoms across grain boundaries, causing the formation of voids and hillocks on the metal [6]. This migration of metal atoms causes microstructural damage to the IDTs, which can lead to shorting of adjacent IDTs.

Further, more extensive hillock formation on metal IDTs ultimately affects the electrical performance of the device. In the case of even higher power levels, catastrophic failure can occur, leading to complete device failure. To overcome this problem, different techniques like epitaxial growth of Al film [7, 8], Cu-Al based metal electrodes [9, 10], multi-layered metal electrodes [4, 11, 12], and Al electrodes with Ni [13] and Ti [9, 14] underlayer have been employed. SAW-induced stress at the interface of a piezoelectric wafer and metal film is higher [15] than in other locations on the metal film. This stress distribution is the prime cause of acousto-migration. Highly oriented Al (111) thin film has been reported to resist acousto-migration on different piezoelectric wafers [16, 17]. Hence in this study, we have explored the preferred oriented growth of Al along (111) crystallographic direction using Ti as an underlayer. The developed preferred oriented Al (111) metallization scheme will provide a solid base for mitigating acousto-migration and provide the framework required to fabricate high-power SAW devices.

2. Experimental details

To achieve oriented Al (111) growth, two different metallization schemes using NiCr (Ni-80%, Cr-20%) and Ti under layers on two different single crystal piezoelectric wafers ST-X Quartz and 42° Y-X black $LiTaO_3$ were used. ST-X Quartz offers near zero first order Temperature Coefficient of Delay (TCD) and is hence used in narrowband IF (< 500 MHz) frequency filtering, whereas 42° Y-X black $LiTaO_3$ offers higher SAW velocity and is thus used for RF frequency filtering application (> 500 MHz) [18].

Before metal deposition, the wafers were thoroughly cleaned using acid and base solutions. Before loading the cleaned wafers into the deposition chamber, a vapor degreaser was used to dry the substrates to remove any moisture content. Next, a dual-gun electron beam evaporation system (Elettrorava) was used for metal thin film deposition. The deposition chamber was evacuated to a base vacuum of ~7×10^{-7} mbar using a combination of an oil-free dry scroll pump and a turbo-molecular pump (Elettrorava). Once the base vacuum was achieved, wafers were heated to the desired temperature with the help of IR lamps attached above the wafer holders. The wafer temperature was monitored with the help of a thermocouple attached on top of the wafer holder. The wafer holder was rotated at a constant speed of 5 rpm in planetary motion for uniform deposition. Finally, the blanket deposition on wafers was performed by varying the deposition temperature and deposition rate of metals.

Table 1. Summary of total samples prepared on ST-X Quartz and 42° Y-X black $LiTaO_3$ wafers

S No.	Metallization scheme	Deposition temperature	
		75 °C	100 °C
		Al Deposition rate (Å/s)	Al Deposition rate (Å/s)
1	NiCr/Al	3, 4, 5, 7, 8, 10	3, 7
2	Ti/Al	3, 4, 5, 7, 8, 10	3, 7

Two different deposition temperatures: 75 °C and 100 °C, were used. NiCr/Ti underlayer and Al (99.99%) metal films were deposited at the same temperature of 75/100 °C. NiCr (100 Å) and Ti (50 Å) deposition rates were maintained at 1 Å/s in all experiments, whereas the deposition rate of Al metal varied from 3 Å/s to 10 Å/s. A total metal thickness of 2650 Å was deposited, and the deposited film thickness was monitored using a quartz crystal microbalance. To identify the suitable deposition conditions to obtain textured Al (111) growth, a total of 32 samples were prepared. A summary of the total samples prepared is given in Table 1.

The crystal structure of deposited metal films was characterized using High-Resolution X-Ray Diffraction (Bruker, D8). The sheet resistance of the deposited films was measured using a four-point probe SR measurement system (Jandel, RM 3000). Surface morphology was characterized by measuring the surface roughness of deposited metal films using a surface profiler (KLA Tencor, D 600) and AFM (Agilent, SPM 5402).

The fabricated SAW devices ultimately have to operate in harsh space environments. In this condition, it becomes essential that the thin metal film be tested under such extreme environmental conditions. Therefore, before patterning the device, a series of space qualification tests were performed on Ti/Al metalized substrates.

3. Results and discussion

3.1 *Sheet Resistance measurement*

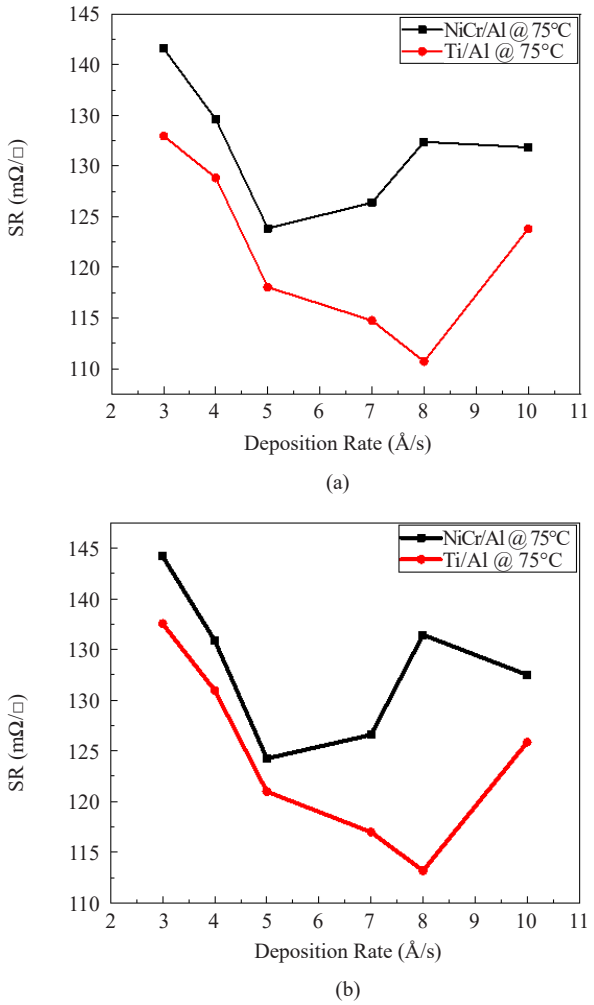

Figure 1. Sheet Resistance (SR) measurement results for different deposition rate of Al. (a) at deposition temperatures 75 °C on ST-X Quartz wafer. (b) at deposition temperatures 75 °C on 42° Y-X black $LiTaO_3$ wafer. Ti (50 Å)/Al (2600 Å), NiCr (100 Å)/Al (2550 Å) were deposited

Figure 1 shows the SR of the NiCr/Al and Ti/Al metallization on two different piezoelectric wafers at a deposition temperature of 75 °C. In both Figure 1(a) and 1(b), Ti/Al metallization shows slightly lower SR values as compared to NiCr/Al metallization. Lower values of SR for Ti/Al metal film imply lower resistive losses during device operation; hence, better device performance with reduced insertion losses is expected [19]. For NiCr/Al metallization scheme on ST-X Quartz wafer, SR value decreased from 141.6 mΩ/sq to 123.9 mΩ/sq corresponding to Al metal deposition rate of 3 Å/s and 5 Å/s respectively at 75 °C deposition temperature. A slight increase in SR from 126.4 mΩ/sq to 132.4 mΩ/sq was observed as the Al deposition rate was increased from 7 Å/s to 8 Å/s at the same temperature.

For the case of Ti/Al metallization scheme on 42° Y-X black $LiTaO_3$ wafer, a decrease in SR value from 137.6 mΩ/sq at 3 Å/s Al deposition rate to 113.2 mΩ/sq at 8 Å/s Al deposition rate was observed which increased to 125.8 mΩ/sq at 10 Å/s Al deposition rate at 75 °C deposition temperature. At 100 °C, the SR value trend was observed to be similar for Ti/Al metallization on both 42° Y-X black $LiTaO_3$ and ST-X Quartz wafers. Grain boundaries are closely located for thin films, and grain size impacts the electrical performance of thin metal films [20]. Therefore, the variation of SR on Al deposition rate can be attributed to the variation in grain size due to different dynamics of thin film growth controlled by deposition rate and deposition temperature.

3.2 *Structural characterization of metalized films*

High Resolution X-ray Diffraction (HR-XRD) measurement is carried out on deposited metallic films to understand how the NiCr and Ti under layer influence the crystalline quality of the Al electrode. Figure (2 & 3) show the coupled 2θ-θ scan of NiCr/Al and Ti/Al metallization at different temperatures. Full HR-XRD scans with 2θ ranging from 30°-90° were performed using a Cu radiation source of ƛ = 1.54 Å. Sharp Al (111) peak corresponding to Face-Centered Cubic (FCC) structure was observed at 2θ = 38.18° dominating other peaks of Al (200) and Al (220). This indicates that Al film growth having (111) preferred orientation is achieved. Here, in our sample the Ti (002) peak is suppressed due to low thickness and very close peak position near Al (111) which is very hard to identify. A slightly poor Al (111) intensity peak was observed on ST-X Quartz wafer as compared to 42° Y-X black $LiTaO_3$ wafer (Figure 2).

The texture quality of Al metallization in different wafers is further evaluated using Full Width Half Maxima (FWHM) of HR-XRD Rocking Curve (RC) analysis along Al (111) plane. Inset of Figure 2(a) and 2(b) shows the FWHM value of rocking curve of 13.38° for NiCr/Al film on 42° Y-X black $LiTaO_3$ wafer was obtained, whereas on ST-X Quartz wafer it was 14.82° for same deposition conditions mentioned in Figure 2(a & b). FWHM values show the better texture quality of Al film on 42° Y-X black $LiTaO_3$ wafer along (111) than ST-X Quartz. The lowest FWHM of 13.20° was obtained for NiCr/Al film on 42° Y-X black $LiTaO_3$ wafer at 75 °C and 7 Å/s Al deposition rate.

Now, the XRD measurement results of Ti/Al metalized films are shown in Figure 3(a & b). The relatively higher Al (111) peak intensity on ST-X Quartz wafer as well as 42° Y-X black $LiTaO_3$ wafer clearly indicates better crystalline quality than the previously deposited NiCr/Al metallization scheme. For Ti/Al film on the 42° Y-X black $LiTaO_3$ wafer with the lowest rocking curve FWHM of 9.68° (Inset of Figure 3(a)) was obtained under the given deposition conditions. Similarly, on the ST-X Quartz wafer, an FWHM of 4.12° was obtained (Inset of Figure 3(b)), which is the lowest among all the deposition conditions. This reduction in FWHM value of rocking curve shows better crystalline quality of Al (111) film on ST-X Quartz with Ti underlayer as compared to NiCr under layer. The lower the FWHM value, the larger the grain size and lesser the number of grain boundaries. This reduction in grain boundaries is desired to arrest acousto-migration and improve device performance at higher power levels.

Hence, Ti under layer is better than that of NiCr under layer. Here, it is clear that acousto-migration in a relatively higher textured sample with a 50 Å Ti under layer will be less than those of the weakly Al (111) textured sample with NiCr layer. It is very well known that the texture quality can greatly influence the power durability and acousto-migration performance of electrodes in SAW devices [21]. High texture is the indicator of intensive dispersive orientation of grains which reduces the extent of grain boundaries, resists acousto-migration and reduces SAW device failure.

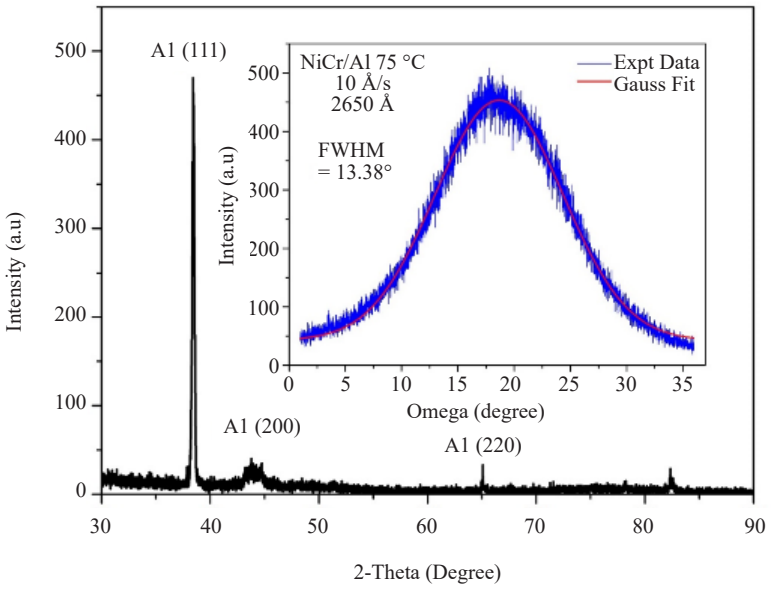

(a)

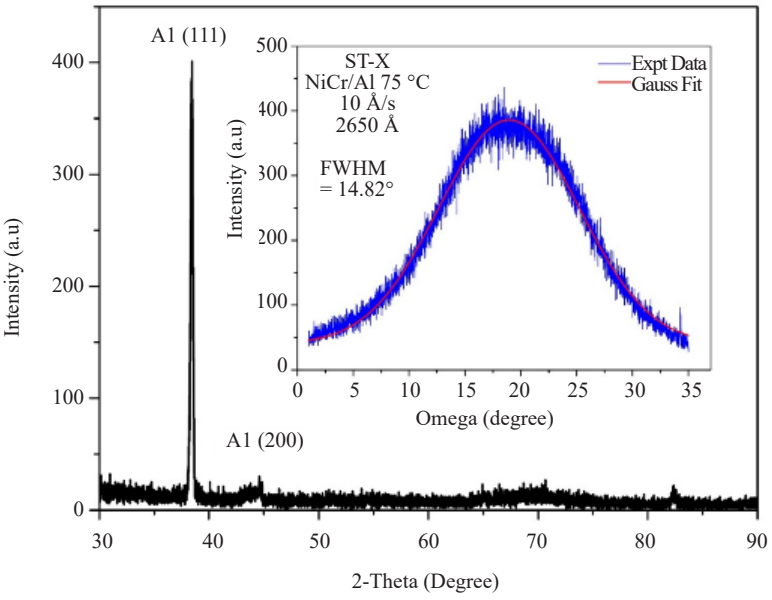

(b)

Figure 2. XRD θ-2θ scan for NiCr/Al film deposited at 75 °C and 7 Å/s Al deposition rate on (a) 42° Y-X black $LiTaO_3$ wafer and on (b) ST-X Quartz wafer. Inset in (a) and (b) shows the rocking curve scan along Al (111) peak

Table 2. Measured average roughness of NiCr/Al film on 42° Y-X black $LiTaO_3$ and Ti/Al film on ST-X Quartz wafer at 100 °C and 7 Å/s Al deposition rate

S. No.	Metallization scheme	Average Roughness as measured from Surface Profiler (Ra) (Å)	Average Roughness as measured from AFM (Ra) (Å)
1	NiCr/Al	18	26
2	Ti/Al	14	20

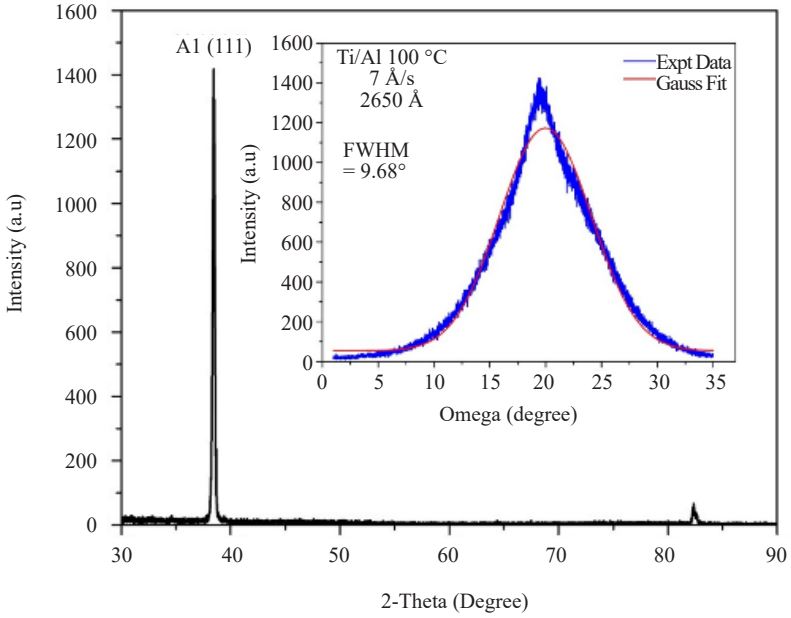

(a)

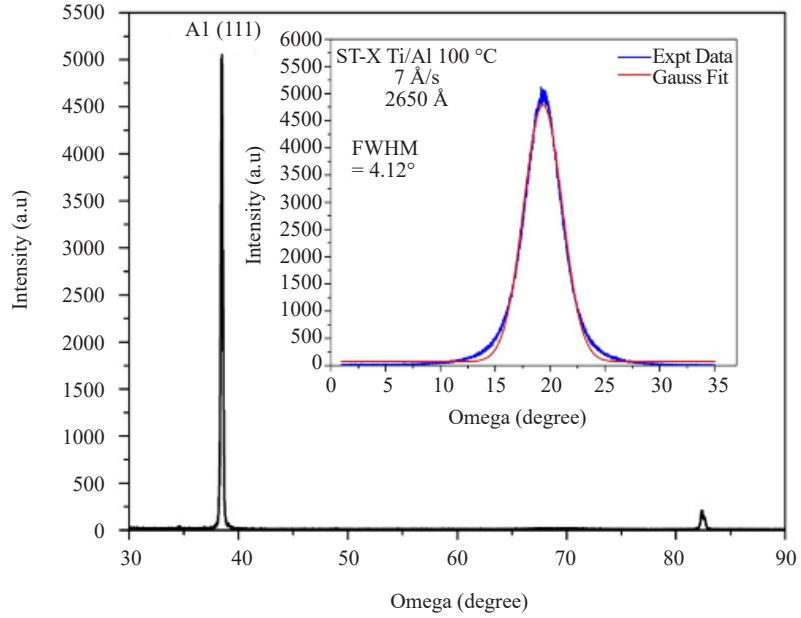

(b)

Figure 3. XRD θ-2θ scan for Ti/Al film deposited at 100 °C and 7 Å/s Al deposition rate on (a) 42° Y-X black $LiTaO_3$ wafer and on (b) ST-X Quartz wafer. Inset in (a) and (b) shows the rocking curve scan along Al (111) peak

3.3 *Surface morphology*

The surface morphology of deposited films was characterized using a surface profiler and AFM. For different metallization schemes on wafers at 100 °C deposition temperature and 7 Å/s Al deposition rate, the average surface roughness (Ra) as measured with both surface profiler and AFM is shown in Table 2. The slight decrease in Ra of Ti/Al film suggests that our Ti/Al film with preferred oriented growth along (111) has better surface morphology and lesser defect density than NiCr/Al metal film (Figure 4).

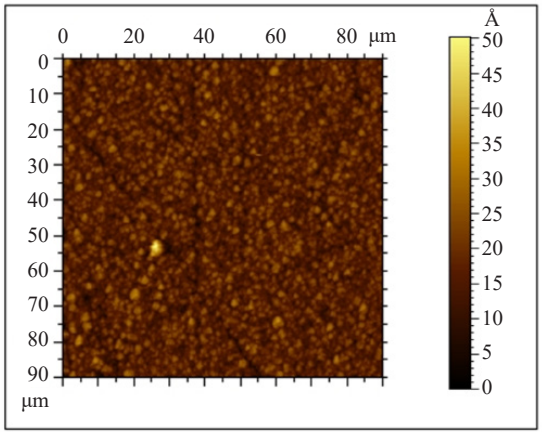

(a)

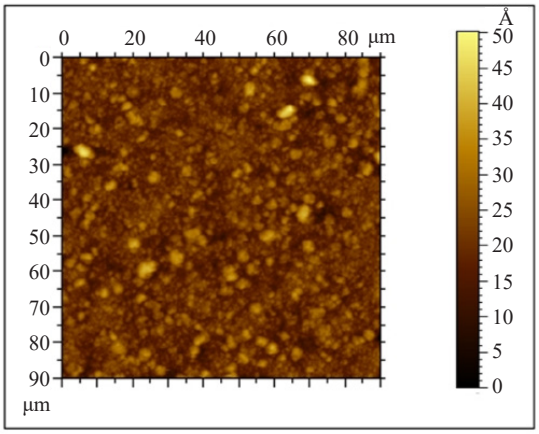

(b)

Figure 4. Image obtained from AFM. (a) Ti/Al film on ST-X Quartz at 100 °C and 7 Å/s Al deposition rate. (b) NiCr/Al film on 42° Y-X black $LiTaO_3$ at 100 °C and 7 Å/s Al deposition rate

3.4 *Qualification tests for space application*

To prove the suitability of Ti/Al thin film for SAW device fabrication to be used for Flight Models (FM) in space, some environmental tests are required to be done. A set of space qualification tests were thus performed on Ti/Al metalized substrates as per the scheme shown in Figure 5.

The metalized wafers were first thoroughly observed under an optical microscope. Then SR measurement was performed on the metalized wafers. After SR measurement, the thermal cycling test was performed as per the conditions mentioned in Table 3. After thermal cycling, again, metalized wafers were examined under an optical microscope, and their SR was measured. SR increased appreciably for Ti/Al metalized wafers on both ST-X Quartz and 42° Y-X black $LiTaO_3$ wafers. This increase in SR after the Thermal Cycling test agrees with our qualified process for NiCr/Al metallization. Table 4 compares SR measurements before and after performing the Thermal Cycling test. Although an increase in SR is observed for Ti/Al metallization for both wafer types, they are well below the upper limit of 600 mΩ/□ for proper device performance. Finally, the adhesion test of the metal film was performed using scotch tape as per MIL-STD-977, Method 4500. After the adhesion test, the metal film did not show any base metal exposure, peel-off, or craters which was evident by the absence of any metal flake on the tape.

Table 3. Thermal cycling test conditions for space qualification test

Test condition	No. of cycles	Temperature range	Dwell time	Transfer time
Temperature cycling	100	-55 °C to +125 °C	10 minutes	1 minute

Table 4. SR measurement results before and after Thermal Cycling test on Ti/Al metallization on ST-X Quartz and 42° Y-X black $LiTaO_3$ wafer under 100 °C and 7 Å/s Al deposition rate

Wafer	SR before Thermal Cycling (mΩ/□)	SR after Thermal Cycling (mΩ/□)
ST-X Quartz	142	194
42° Y-X black $LiTaO_3$	139	190

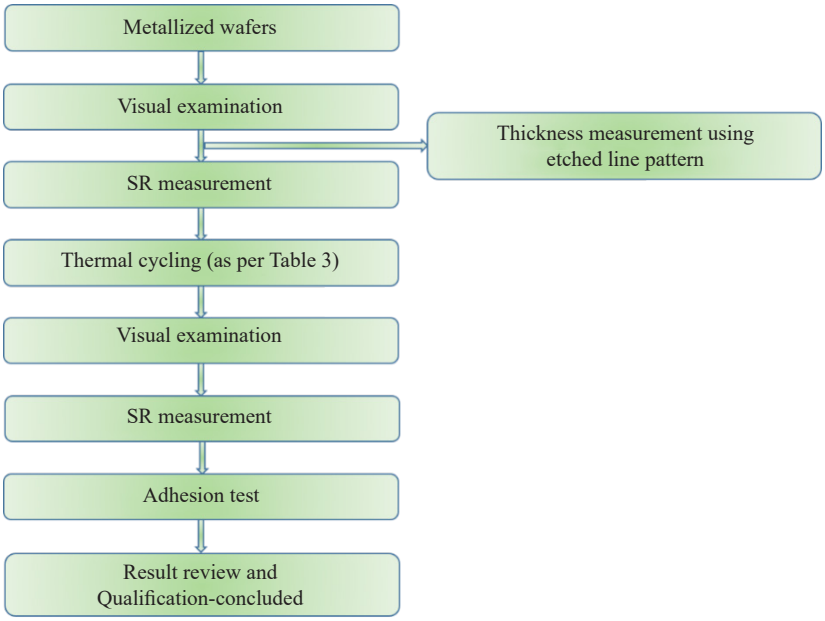

Figure 5. Flowchart for space qualification tests for metallization process

4. Conclusion

In this work, Ti/Al (2650 Å) metallization scheme was explored as compared to NiCr/Al (2650 Å) metallization to enhance the acousto-migration resistance of metal atoms across grain boundaries. Electron Beam evaporation was used for metal thin film deposition. ST-X Quartz and 42° Y-X black $LiTaO_3$ wafers were used to deposit thin metal films. Deposition was performed at 75 °C and 100 °C substrate temperatures. Using an ultrathin underlayer of Ti (50 Å), Al (111) metal film was grown on an ST-X Quartz wafer with high crystalline quality. The crystalline quality was measured from the Rocking curve analysis on Al (111) peak in the XRD scan. Our studies show that a deposition rate of 1 Å/s for Ti and 7 Å/s for Al at a deposition temperature of 100 °C gives a highly preferred oriented Al (111) film on ST-X Quartz wafer. The surface morphology of the deposited film was characterized in terms of surface roughness, and its electrical characterization was performed using a four-point probe sheet resistance measurement. A combination of surface profiler and AFM was used to visually inspect the defects formed on the metal films during deposition. A set of

space qualification tests were also performed to establish the trustworthiness of Ti/Al metalized wafers for FM device fabrication. It is concluded that the SAW devices with highly textured Al electrodes on 50 Å Ti under layer indicate significant enhancements in acousto-migration resistance, the reductions in overall and extent of grain boundaries in the electrodes. Therefore, an ultrathin Ti under layer is suitable for growing the highly textured Al metallization to be used for fabricating SAW devices for high power applications.

Acknowledgement

We thank Group Head MEG, Deputy Director ESSA, and Director SAC for their encouragement of this study. We are also thankful to Microelectronics Group, SAC, for technical support.

Conflict of interest

All authors declare that they have no conflicts of interest.

References

[1] Balysheva OL. SAW filters for mobile communications: Achievements and prospects. *2019 Wave Electronics and its Application in Information and Telecommunication Systems (WECONF)*. 2019. p. 1-4.
[2] Rutkowski R. *The ultimate guide to SAW Filters*. Available from: https://blog.bliley.com/the-ultimate-guide-to-saw-filters [Assessed 28th September 2021].
[3] Balysheva OL. SAW filters substrates for 5G filters. In *2022 Wave Electronics and its Application in Information and Telecommunication Systems (WECONF)*. IEEE; 2022. p. 1-7.
[4] Su R, Fu S, Shen J, Lu Z, Xu H, Yang M, et al. Power durability enhancement and failure analysis of TC-SAW filter with Ti/Cu/Ti/Cu/Ti electrodes. *IEEE Transactions on Device and Materials Reliability*. 2021; 21(3): 365-371.
[5] Hesjedal T, Mohanty J, Kubat F, Ruile W, Reindl LM. A microscopic view on acoustomigration. *IEEE Transactions on Ultrasonics, Ferroelectrics, and Frequency Control*. 2005; 52(9): 1584-1593.
[6] Pekarcikova M, Hofmann M, Menzel S, Schrnidt H, Gemming T, Wetzig K. Investigation of high power effects on Ti/Al and Ta-Si-N/Cu/Ta-Si-N electrodes for SAW devices. *IEEE Transactions on Ultrasonics, Ferroelectrics, and Frequency Control*. 2005; 52(5): 911-917.
[7] Kimura N, Nakano M, Sato K. High power-durable and low loss single-crystalline Al/Ti electrodes for RF SAW devices. In *1998 IEEE Ultrasonics Symposium. Proceedings (Cat. No. 98CH36102)*. IEEE; 1998. p. 315-318.
[8] Sakurai A, Nakanishi H, Yoshino Y, Katayama Y. Epitaxially grown aluminum film for high-power surface acoustic wave devices. *Proceedings of 1995 Japan International Electronic Manufacturing Technology Symposium*. IEEE; 1995. p. 383-386.
[9] Fu S, Wang W, Xiao L, Lu Z, Li Q, Song C, et al. Texture-enhanced Al-Cu electrodes on ultrathin Ti buffer layers for high-power durable 2.6 GHz SAW filters. *AIP Advances*. 2018; 8(4): 045212. Available from: doi: 10.1063/1.5017091.
[10] Spindler M, Menzel SB, Eckert J, Eggs C. Influence of Al on resistance and power durability of Cu-based SAW metallizations. *IOP Conference Series Materials Science and Engineering*. 2010; 8(1): 012013. Available from: doi: 10.1088/1757-899X/8/1/012013.
[11] Takayama R, Nakanishi H, Hashimoto K. Impact of composition and structure of al alloy electrodes to power durability of SAW devices. In *2014 IEEE International Ultrasonics Symposium*. IEEE; 2014. p. 886-892.
[12] Li Q, Fu S, Lu Z, Qian L, Wang R, Chen T, et al. Behavior of Al/Cu/Ti electrodes in surface acoustic wave filter at high power. *Current Applied Physics*. 2019; 19(4): 363-369.
[13] Li Q, Fu SL, Song C, Wang GY, Zeng F, Pan F. Improved resistance to electromigration and acoustomigration of Al interdigital transducers by Ni underlayer. *Rare Metals*. 2018; 37(10): 823-830.
[14] Liu H, Zeng F, Tang G, Wang G, Song C, Pan F. Significant enhancement in electromigration resistance and texture of aluminum films using an ultrathin titanium underlayer. *Acta Materialia*. 2013; 61(12): 4619-4624.

[15] Kubat F, Ruile W, Rosler U, Ruppel CC, Reindl LM. Calculation of the SAW-induced stress distributions in an electrode of a SAW-device on $LiTaO_3$. In *IEEE Ultrasonics Symposiu*. IEEE; 2004. p. 437-440.
[16] Nakagawara O, Saeki M, Tsubaki N, Taniguchi N, Ikada K, Watanabe M, et al. High power durable SAW antenna duplexers for W-CDMA with epitaxially grown aluminum electrodes. In *2002 IEEE Ultrasonics Symposium*. IEEE; 2002. p. 43-46.
[17] Nakagawara O, Saeki M, Teramoto A, Hasegawa M, Ieki H. High power durable SAW filter with epitaxial aluminium electrodes on 3 8.5 rotated YX $LiTaO_3$ by two-step process sequence in titanium intermediate layer. In *IEEE Symposium on Ultrasonics*. IEEE; 2003. p. 1734-1737.
[18] *Introduction to SAW Filter Theory & Design Techniques*. Available from: https://www.apitech.com/globalassets/documents/rf2m-us/white-paper---saw-filter-2018.pdf [Assessed 1st August 2022].
[19] Kadota M, Nakao T, Taniguchi N, Takata E, Mimura M, Nishiyama K, et al. SAW substrate for duplexer with excellent temperature characteristics and large reflection coefficient realized by using flattened SiO_2 film and thick heavy metal film. In *2006 IEEE MTT-S International Microwave Symposium Digest*. IEEE; 2006. p. 382-385.
[20] Mayadas AF, Shatzkes M. Electrical-resistivity model for polycrystalline films: the case of arbitrary reflection at external surfaces. *Physical Review B*. 1970; 1(4): 1382. Available from: doi: 10.1103/PhysRevB.1.1382.
[21] Nüssl R, Jewula T, Ruile W, Sulima T, Hansch W. Correlation between texture and mechanical stress durability of thin aluminum films. *Thin Solid Films*. 2014; 556: 376-380.